ISSN (Print) : 2320 – 3765
ISSN (Online): 2278 – 8875

International Journal of Advanced Research in Electrical, Electronics and Instrumentation Engineering

(An ISO 3297: 2007 Certified Organization)

Vol. 5, Issue 6, June 2016

Performance Improvement of Renewable Energy Systems through Active Power Filters for Meeting the Energy Demand and Power Quality Improvement

M.B.Hemanth Kumar[1], M.Chandrashekhar[2]

Assistant Professor, Dept. of EEE, Annamacharya Institute of Technology and Sciences, Hyderabad, India[1]

Assistant Professor, Dept. of EEE, Annamacharya Institute of Technology and Sciences, Hyderabad, India[2]

ABSTRACT: Renewable generation affects power quality due to its nonlinearity, since solar generation plants and wind power generators must be connected to the grid through high-power static PWM converters. The non uniform nature of power generation directly affects voltage regulation and creates voltage distortion in power systems. This new scenario in power distribution systems will require more sophisticated compensation techniques. An active power filter implemented with a four-leg voltage-source inverter using a predictive control scheme is presented. This project presents the mathematical model of the 4L-VSI and the principles of operation of the proposed predictive control scheme, including the design procedure.

KEYWORDS: Voltage source inverter, Power quality, PWM converter, Predictive control scheme,

I. INTRODUCTION

Renewable generation affects power quality due to its nonlinearity, since solar generation plants and wind power generators must be connected to the grid through high-power static PWM converters [1]. The non uniform nature of power generation directly affects voltage regulation and creates voltage distortion in power systems. This new scenario in power distribution systems will require more sophisticated compensation techniques. Although active power filters implemented with three-phase four-leg voltage-source inverters (4L-VSI) have already been presented in the technical literature [2]–[6], the primary contribution of this paper is a predictive control algorithm designed and implemented specifically for this application. Traditionally, active power filters have been controlled using pre tuned controllers, such as PI-type or adaptive, for the current as well as for the dc-voltage loops [7], [8].

PI controllers must be designed Based on the equivalent linear model, while predictive controllers use the nonlinear model, which is closer to real operating conditions. So far, implementations of predictive control in power convertershave been used mainly in induction motor drives [9]–[16]. In the case of motor drive applications, predictive controlrepresents a very intuitive control scheme that handles multivariable characteristics, simplifies the treatment of dead-time compensations, and permits pulse-width modulator replacement. However, these kinds of applications present disadvantages related to oscillations and instability created from unknown load parameters [15].

These power quality concerns made the power engineers to think about the devices which reduces the harmonics in the supply line [E,F].Such devices are known as active power filter/power conditioners which are capable of current/voltage harmonic compensation. Active power filters are classified into shunt , series and hybrid active power filters which can deal with various power quality issues [A,E]. Nowadays power quality issues in single One advantage of the proposed algorithm is that it fits well in active power filter applications, since the power converter output parameters are well known [17]. These output parameters are obtained from the converter output ripple filter and the power system equivalent impedance. The converter output ripple filter is part of the active power filter design and the power system impedance is obtained from well-known standard procedures [18], [19]. In the case of unknown system impedance parameters, an estimation method can be used to derive an accurate *R–L*

ISSN (Print) : 2320 – 3765
ISSN (Online): 2278 – 8875

International Journal of Advanced Research in Electrical, Electronics
(A

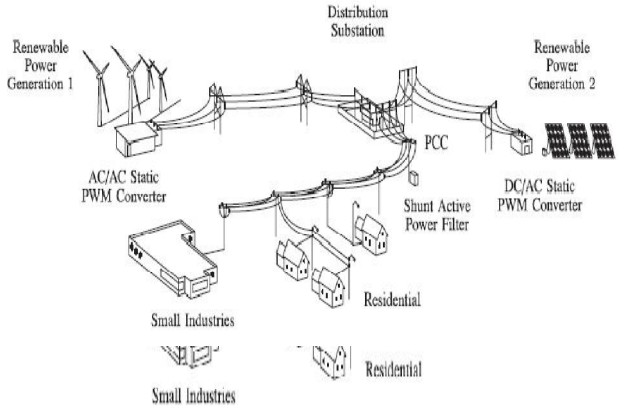

Fig. 1 Stand-alone hybrid power generation system with a shunt active power filter.

equivalent impedance model of the system [20]. This paper presents the mathematical model of the 4L-VSI and the principles of operation of the proposed predictive control scheme, including the design procedure.

II. BASIC AND FOUR-LEG CONVERTER MODEL

Fig. 1 shows the configuration of a typical power distribution system with renewable power generation. It consists of various types of power generation units and different types of loads. Renewable sources, such as wind and sunlight, are typically used to generate electricity for residential users and small industries. Both types of power generation use ac/ac and dc/ac static PWM converters for voltage conversion and battery banks for long term energy storage. These converters perform maximum power point tracking to extract the maximum energy possible from wind and sun. The electrical energy consumption behavior is random and unpredictable, and therefore, it may be single- or three-phase, balanced or unbalanced, and linear or nonlinear. An active power filter is connected in parallel at the point of common coupling to compensate current harmonics, current unbalance, and reactive power. It is composed by an electrolytic capacitor, a four-leg PWM converter, and a first- order output ripple filter.

Zf, and the load impedance *ZL* . Based on topologies, they are two kinds of active filter such as current source and voltage source active filters. Current source active filters (CSAF) employ an inductor as the DC energy storage deviceSo in this project we are using the shunt active power filter.The four-legPWMconverter topology is shown in Fig. 3. This converter topology is similar to the conventional three-phase converter with the fourth leg connected to the neutral bus of the system. The fourth leg increases switching states from 8 (23) to 16 (24), improving control flexibility and output voltage quality [21], and is suitable for current unbalanced compensation. The voltage in any leg *x* of the converter, measured from the neutral point (*n*), can be expressed in terms of switching states, as follows:

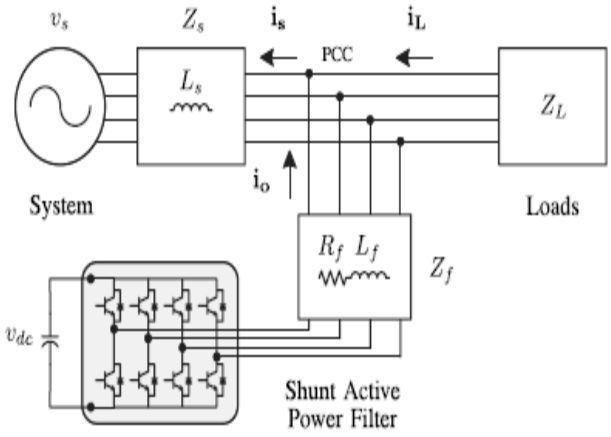

Fig. 2 This circuit considers the power system equivalent impedance *Zs*, the converter output ripple filter impedance

ISSN (Print) : 2320 – 3765
ISSN (Online): 2278 – 8875

International Journal of Advanced Research in Electrical, Electronics and Instrumentation Engineering

(An ISO 3297: 2007 Certified Organization)

Vol. 5, Issue 6, June 2016

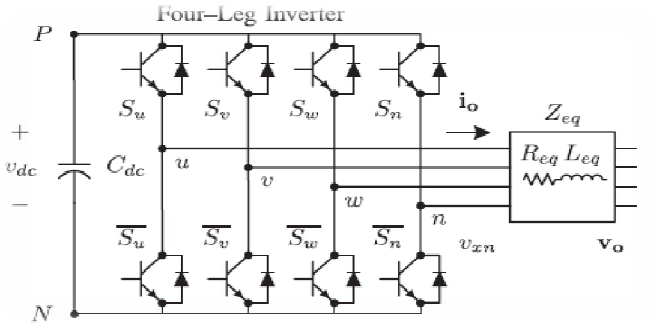

Fig. 3 Two-level four-leg PWM-VSI topology.

$$V_{xn} = S_x - S_n V_{dc}$$
$$X = u,v,w,n. \quad (1)$$

The mathematical model of the filter derived from the equivalent circuit shown in Fig. 2 is

$$V_o = V_{xn} - R_{eq} i_o - L_{eq} \frac{di_o}{dt} \quad (2)$$

where*R*eq and *L*eq are the 4L-VSI output parameters expressed as Thevenin impedances at the converter output terminals *Z*eq . Therefore, the Thevenin equivalent impedance is determined by a series connection of the ripple filter impedance *Zf*and a parallel arrangement between the system equivalent impedance *Zs*and the load impedance *ZL*

$$Z_{eq} = \frac{Z_s Z_L}{Z_s + Z_L} + Z_f \approx Z_s + Z_f \quad (3)$$

For this model, it is assumed that *ZL* _ *Zs*, that the resistive part of the system's equivalent impedance is neglected, and that the series reactance is in the range of 3–7% p.u., which is an acceptable approximation of the real system. Finally, in (2) *R*eq = *Rf*and*L*eq = *Ls*+ *Lf* .

III. DIGITAL PREDICTIVE CURRENT CONTROL

The block diagram of the proposed digital predictive current control scheme is shown in Fig. 4. This control scheme is basically an optimization algorithm and, therefore, it has to be implemented in a microprocessor. Consequently, the analysis has to be developed using discrete mathematics in order to consider additional restrictions such as time delays and approximations [10], [22]–[27]. The main characteristic of predictive control is the use of the system model to predict the future behavior of the variables to be controlled. The controller uses this information to select the optimum switching state that will be applied to the power converter, according to predefined optimization criteria. The predictive control algorithm is easy to implement and to understand, and it can be implemented with three main blocks, as shown in Fig. 4.

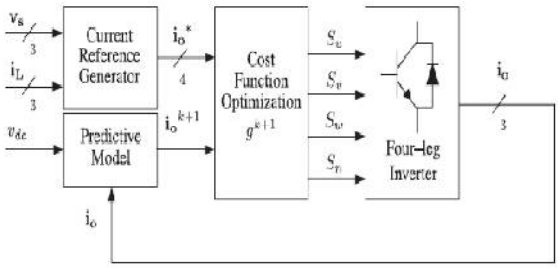

Fig. 4 Proposed predictive digital current control block diagram.

1) Current Reference Generator: This unit is designed to generate the required current reference that is used to compensate the undesirable load current components. In this case, the system voltages, the load currents, and the dc-voltage converter are measured, while the neutral output current and neutral load current are generated directly from these signals (IV).

ISSN (Print) : 2320 – 3765
ISSN (Online): 2278 – 8875

International Journal of Advanced Research in Electrical, Electronics and Instrumentation Engineering

(An ISO 3297: 2007 Certified Organization)

Vol. 5, Issue 6, June 2016

2) Prediction Model: The converter model is used to predict the output converter current. Since the controller operates in discrete time, both the controller and the system model must be represented in a discrete time domain [22]. The discrete time model consists of a recursive matrix equation that represents this prediction system. This means that for a given sampling time *Ts*, knowing the converter switching states and control variables at instant *kTs*, it is possible to predict the next states at any instant [*k* + 1]*Ts*.Due to the first-order nature of the state equations that describe the model in (1)–(2), a sufficiently accurate first-order approximation of the derivative is considered in this project

$$\frac{dx}{dt} \approx \frac{X[K+1]+X[K]}{T_S} \qquad (4)$$

The 16 possible output current predicted values can be obtained from (2) and (4) as.

$$i_o\,[K+1] = \frac{T_s}{L_{eq}}\left(v_{xn}[K] - V_o[K]\right) + \left(1 - \frac{R_{eq}T_s}{L_{eq}}\right) i_o[K] \qquad (5)$$

As shown in (5), in order to predict the output current **io**at the instant (*k* + 1), the input voltage value **vo**and the converter output voltage *vxN*, are required. The algorithm calculates all 16 values associated with the possible combinations that the state variables can achieve.

3) Cost Function Optimization: In order to select the optimal switching state that must be applied to the power converter, the 16 predicted values obtained for **io**[*k* + 1] are compared with the reference using a cost function *g*, as follows:

$$g[K+1] = (i_{ou}{}^*[K+1] - i_{ou}[K+1])^2 + (i_{ov}{}^*[K+1] - i_{ov}[K+1])^2 + (i_{ow}{}^*[K+1] - i_{ow}[K+1])^2 + (i_{on}{}^*[K+1] - i_{on}[K+1])^2 \qquad (6)$$

The output current (**io**) is equal to the reference (**i∗o**) when $g = 0$. Therefore, the optimization goal of the cost function isto achieve a *g* value close to zero. The voltage vector **vxN**that minimizes the cost function is chosen and then applied at thenext sampling state. During each sampling state, the switchingstate that generates the minimum value of *g* is selected from the16 possible function values. The algorithm selects the switchingstate that produces this minimal value and applies it to theconverter during the *k* + 1 state.

IV. CURRENT REFERENCE GENERATION

A *dq*-based current reference generator scheme is used to obtain the active power filter current reference signals. This scheme presents a fast and accurate signal tracking capability. This characteristic avoids voltage fluctuations that deteriorate the current reference signal affecting compensation performance [28]. The current reference signals are obtained from the corresponding load currents as shown in Fig. 5. This module calculates the reference signal currents required by the converter to compensate reactive power, current harmonic, and current imbalance. The displacement power factor (sin $\varphi(L)$) and the maximum total harmonic distortion of the load (THD(L)) defines the relationships between the apparent power required by the active power filter, with respect to the load, as shown

$$\frac{S_{APF}}{S_L} = \frac{\sqrt{\sin \emptyset_{(L)} + THD_{(L)}{}^2}}{\sqrt{1 + THD_{(L)}{}^2}} \qquad (7)$$

where the value of THD(L) includes the maximum compensable harmonic current, defined as double the sampling frequency *fs*. The frequency of the maximum current harmonic component that can be compensated is equal to one half of the converter switching frequency. The *dq*-based scheme operates in a rotating reference frame; therefore, the measured currents must be multiplied by the sin(*wt*) and cos(*wt*) signals. By using *dq*-transformation, the *d* current component is synchronized with the corresponding phase-to-neutral system voltage, and the *q* current component is phase-shifted by 90◦.

ISSN (Print) : 2320 – 3765
ISSN (Online): 2278 – 8875

International Journal of Advanced Research in Electrical, Electronics and Instrumentation Engineering

(An ISO 3297: 2007 Certified Organization)

Vol. 5, Issue 6, June 2016

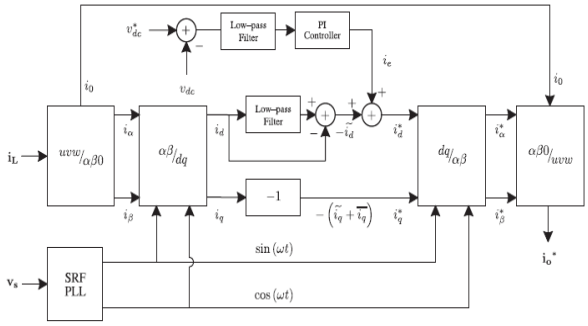

Fig. 5 *dq*-based current reference generator block diagram.

The sin(*wt*) and cos(*wt*) synchronized reference signals are obtained from a synchronous reference frame (SRF) PLL [29]. The SRF-PLL generates a pure sinusoidal waveform even when the system voltage is severely distorted. Tracking errors are eliminated, since SRF-PLLs are designed to avoid phase voltage unbalancing, harmonics (i.e., less than 5% and 3% in fifth and seventh, respectively), and offset caused by the nonlinear load conditions and measurement errors [30]. Equation (8) shows the relationship between the real currents *iLx*(*t*) (*x* = *u*, *v*,*w*) and the associated *dq*components (*id* and *iq*)

$$\begin{bmatrix} i_d \\ i_q \end{bmatrix} = \sqrt{\frac{2}{3}} \begin{bmatrix} \sin wt & \cos wt \\ -\cos wt & \sin wt \end{bmatrix} \begin{bmatrix} 1 & -\frac{1}{2} & -\frac{1}{2} \\ 0 & \frac{\sqrt{3}}{2} & -\frac{\sqrt{3}}{2} \end{bmatrix} \begin{bmatrix} i_{Lu} \\ i_{Lv} \\ i_{Lw} \end{bmatrix} \quad (8)$$

Alow-pass filter (LFP) extracts the dc component of the phase currents *id* to generate the harmonic reference components −_*id* . The reactive reference components of the phase-currents are obtained by phase-shifting the corresponding ac and dc components of *iq*by 180◦. In order to keep the dc-voltage constant, the amplitude of the converter reference current must be modified by adding an active power reference signal *ie*with the *d*-component, as will be explained in Section IV-A. The resulting signals *i*∗*d*and*i*∗*q*are transformed back to a three-phase system by applying the inverse Park and Clark transformation, as shown in (9). The cutoff frequency of the LPF used in this project is 20 Hz The current that flows through the neutral of the load is compensated by injecting the same instantaneous value obtainedthird-order harmonic content, and system current imbalance (withrespect to positive sequence of the system current, *is*,1).from the phase-currents, phase-shifted by 180◦, as shown next.

$$\begin{bmatrix} {i_{ou}}^* \\ {i_{ov}}^* \\ {i_{ow}}^* \end{bmatrix} = \sqrt{\frac{2}{3}} \begin{bmatrix} \frac{1}{\sqrt{2}} & 1 & 0 \\ \frac{1}{\sqrt{2}} & -\frac{1}{2} & \frac{\sqrt{3}}{2} \\ \frac{1}{\sqrt{2}} & -\frac{1}{2} & -\frac{\sqrt{3}}{2} \end{bmatrix} * \begin{bmatrix} 1 & 0 & 0 \\ 0 & \sin wt & -\cos wt \\ 0 & \cos wt & \sin wt \end{bmatrix} \begin{bmatrix} i_o \\ {i_a}^* \\ {i_q}^* \end{bmatrix} \quad (9)$$

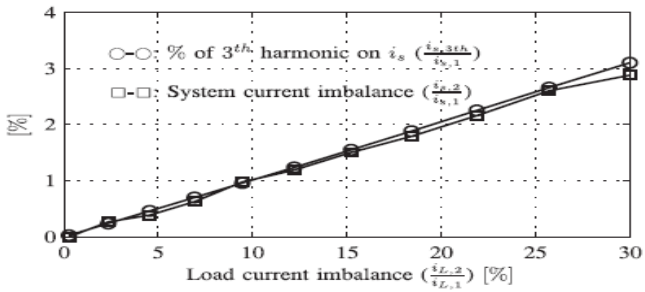

Fig. 6 Relationship between permissible unbalance load currents, the corresponding

$$i_{on}{}^* = -(i_{Lu} + i_{Lv} + i_{Lw})$$

ISSN (Print) : 2320 – 3765
ISSN (Online): 2278 – 8875

International Journal of Advanced Research in Electrical, Electronics and Instrumentation Engineering

(An ISO 3297: 2007 Certified Organization)

Vol. 5, Issue 6, June 2016

One of the major advantages of the *dq*-based current reference generator scheme is that it allows the implementation of a linear controller in the dc-voltage control loop. However, one important disadvantage of the *dq*-based current reference frame algorithm used to generate the current reference is that a secondorder harmonic component is generated in *id* and *iq*under unbalanced operating conditions. The amplitude of this harmonic depends on the percent of unbalanced load current (expressed as the relationship between the negative sequence current *iL*,2 and the positive sequence current *iL*,1). The second-order harmonic cannot be removed from *id* and *iq*, and therefore generates a third harmonic in the reference current when it is converted back to abc frame [31]. Fig. 6 shows the percent of system current imbalance and the percent of third harmonic system current, in function of the percent of load current imbalance. Since the load current does not have a third harmonic, the one generated by the active power filter flows to the power system.

DC-Voltage Control

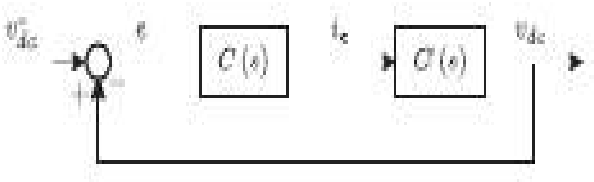

Fig. 7DC-voltage control block diagram.

The dc-voltage converter is controlled with a traditional PI controller. This is an important issue in the evaluation, sine the cost function (6) is designed using only current references, in order to avoid the use of weighting factors. Generally, these weighting factors are obtained experimentally, and they are not well defined when different operating conditions are required. Additionally, the slow dynamic response of the voltage across the electrolytic capacitor does not affect the current transient response. For this reason, the PI controller represents a simple and effective alternative for the dc-voltage control.

The dc-voltage remains constant (with a minimum value of $\sqrt{6}v_s rms$)until the active power absorbed by the converter decreases to a level where it is unable to compensate for its losses. The active power absorbed by the converter is controlled by adjusting the amplitude of the active power reference signal *ie*, which is in phase with each phase voltage. In the block diagram shown in Fig. 5, the dc-voltage *v*dc is measured and then compared with a constant reference value *v*∗dc. The error (*e*) is processed by a PI controller, with two gains, *Kp*and*Ti*. Both gains are calculated according to the dynamic response requirement. Fig. 7 shows that the output of the PI controller is fed to the dc-voltage transfer function *Gs*, which is represented by a first-order system (11)

$$G(s) = \frac{v_{dc}}{i_e} = \frac{3}{2}\frac{K_p v_s\sqrt{2}}{C_{dc}v_{dc}^*} \quad (10)$$

The equivalent closed-loop transfer function of the given system with a PI controller (12) is shown in (13)

$$C(s) = K_p\left(1 + \frac{1}{T_i.S}\right) \quad (11)$$

$$\frac{v_{dc}}{i_e} = \frac{\frac{{w_n}^2}{n}.(s+a)}{s^2+2(w_n.s+{w_n}^2} \quad (12)$$

Since the time response of the dc-voltage control loop does not need to be fast, a damping factor ζ = 1and a natural angular peed ωn= $2\pi \cdot 100$ rad/s are used to obtain a critically damped response with minimal voltage oscillation. The corresponding integral time *Ti* = 1/*a* (13) and proportional gain *Kp*can be calculated as

$$\zeta = \sqrt{\frac{3}{8}\frac{K_p v_s\sqrt{2}T_i}{C_{dc}v_{dc}^*}} \quad (13)$$

$$w_n = \sqrt{\frac{3}{2}\frac{K_p v_s\sqrt{2}}{C_{dc}v_{dc}^* T_i}} (14)$$

ISSN (Print) : 2320 – 3765
ISSN (Online): 2278 – 8875

International Journal of Advanced Research in Electrical, Electronics and Instrumentation Engineering

(An ISO 3297: 2007 Certified Organization)

Vol. 5, Issue 6, June 2016

V. SIMULATION RESULTS

A simulation model for the three-phase four-leg PWM converter with the parameters shown in Table I has been developed usingMATLAB-Simulink. The objective is to verify the current harmonic compensation effectiveness of the proposed control scheme under different operating conditions. A six-pulse rectifier was used as a nonlinear load. The proposed predictive control algorithm was programmed using an S-function block that allows simulation of a discrete model that can be easily implemented in a real-time interface (RTI) on the dSPACE DS1103 R&D control board. Simulations were performed considering a 20 [μs] of sample time. In the simulated results shown in Fig. 8, the active filter starts to compensate at $t = t1$. At this time, the active power filter injects an output current *iou*to compensate current harmonic components, current unbalanced, and neutral current simultaneously.

variable	Description	Value
V_s	Source voltage	55[v]
f	System frequency	50[Hz]
V_{dc}	dc-voltage	162[v]
C_{dc}	dc capacitor	2200[µF] (2.0 pu)
L_f	Filter inductor	5.0[mH] (0.5 pu)
R_f	Internal resistance within L_f	0.6[Ω]
T_s	Sampling time	20[µs]
T_e	Execution time	16[µs]

Table. 1: Specification paramerers.

During compensation, the system currents **is** show sinusoidal waveform, with low total harmonic distortion (THD = 3.93%). At $t = t2$, a three-phase balanced load step change is generated from 0.6 to 1.0 p.u.

The compensated system currents remain sinusoidal despite the change in the load current magnitude. Finally, at $t = t3$, a single-phase load step change is introduced in phase *u* from 1.0 to 1.3 p.u., which is equivalent to an 11% current imbalance.As expected on the load side, a neutral current flows through the neutral conductor (*iLn*), but on the source side, no neutral current is observed (*isn*). Simulated results show that the proposed control scheme effectively eliminates unbalanced currents.

ISSN (Print) : 2320 – 3765
ISSN (Online): 2278 – 8875

International Journal of Advanced Research in Electrical, Electronics and Instrumentation Engineering

(An ISO 3297: 2007 Certified Organization)

Vol. 5, Issue 6, June 2016

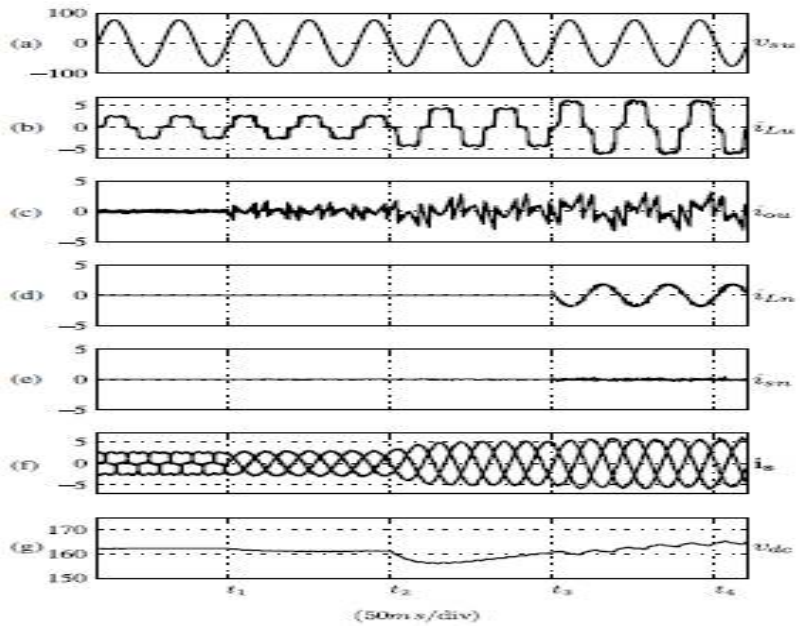

Figure. 8. Simulated waveforms of the proposed control scheme. (a) Phase to neutral source voltage. (b) Load Current. (c) Active power filter output current. (d) Load neutral current. (e) System neutral current. (f) System currents. (g) DC voltage converter.

Additionally, Fig. 8 shows that the dc-voltage remains stable throughout the whole active power filter operation.

The compensation effectiveness of the active power filter is corroborated in a 2 kVA experimental setup. A six-pulse rectifier was selected as a nonlinear load in order to verify the effectiveness of the current harmonic compensation. A step load change was applied to evaluate the transient response of the dcvoltage loop. Finally, an unbalanced load was used to validate the performance of the neutral current compensation. An average switching frequency of 4.64 kHz is obtained.

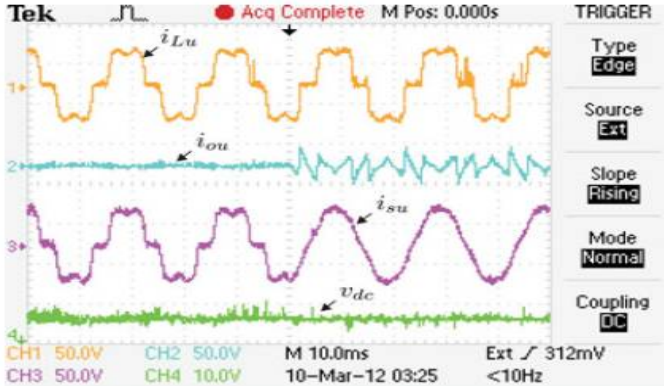

(a)

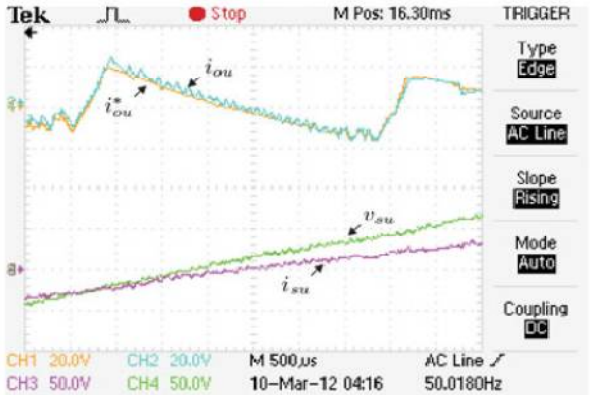

(b)

ISSN (Print) : 2320 – 3765
ISSN (Online): 2278 – 8875

International Journal of Advanced Research in Electrical, Electronics and Instrumentation Engineering

(An ISO 3297: 2007 Certified Organization)

Vol. 5, Issue 6, June 2016

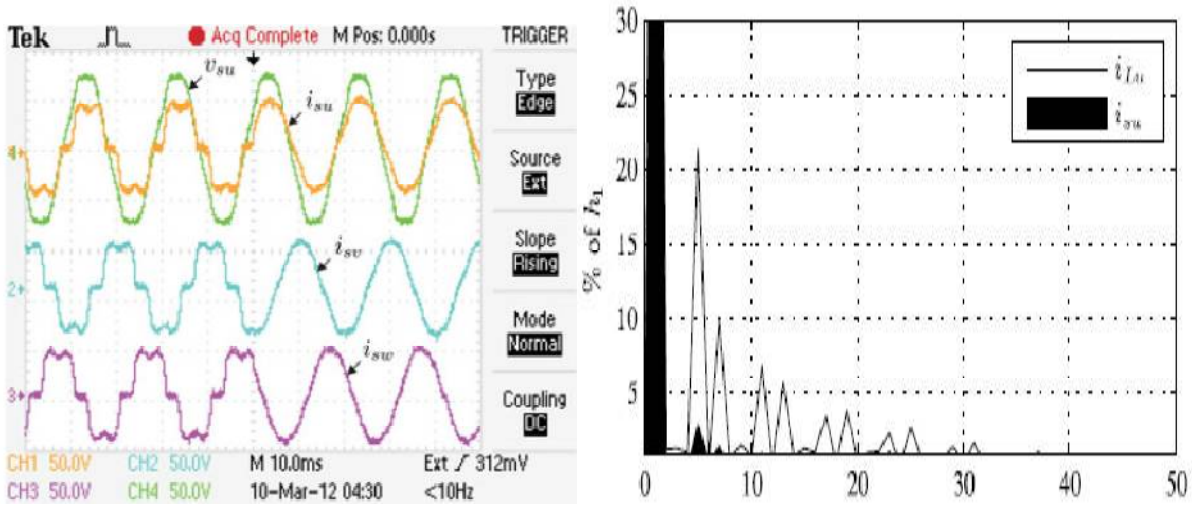

(c) (d)

Figure. 9. Experimental transient response after APF connection. (a) Load Current *iLu*, active power filter current *iou*, (b)dc-voltage converter *v*dc , and system current *isu*. Associated frequency spectrum. (c) Voltage and system waveforms, *vsu*and*isu* ,*isv* , *isw*. (d) Current reference signals *i*∗*ou*, and active power filter current *iou*(tracking characteristic).

Fig. 9 showsthe transient response of the compensation scheme. Fig. 9(a) shows that the line current becomes sinusoidal when the active power filter starts compensation, and the dc-voltage behaves as expected. Experimental results shown in Fig. 9(b) indicate that the total harmonic distortion of the line current (THD*i*) is reduced from 27.09% to 4.54%. This is a consequence of the good tracking characteristic of the current references, as shown in Fig. 9(d).

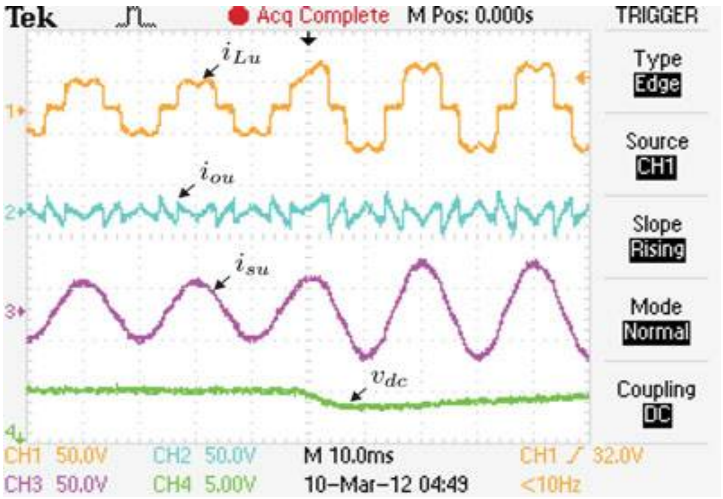

Figure. 10. Experimental results for step load change (0.6 to 1.0 p.u.). Load Current *iLu*, active power filter current *iou*, system current *isu*, and dc-voltage converter *v*dc .

ISSN (Print) : 2320 – 3765
ISSN (Online): 2278 – 8875

International Journal of Advanced Research in Electrical, Electronics and Instrumentation Engineering

(An ISO 3297: 2007 Certified Organization)

Vol. 5, Issue 6, June 2016

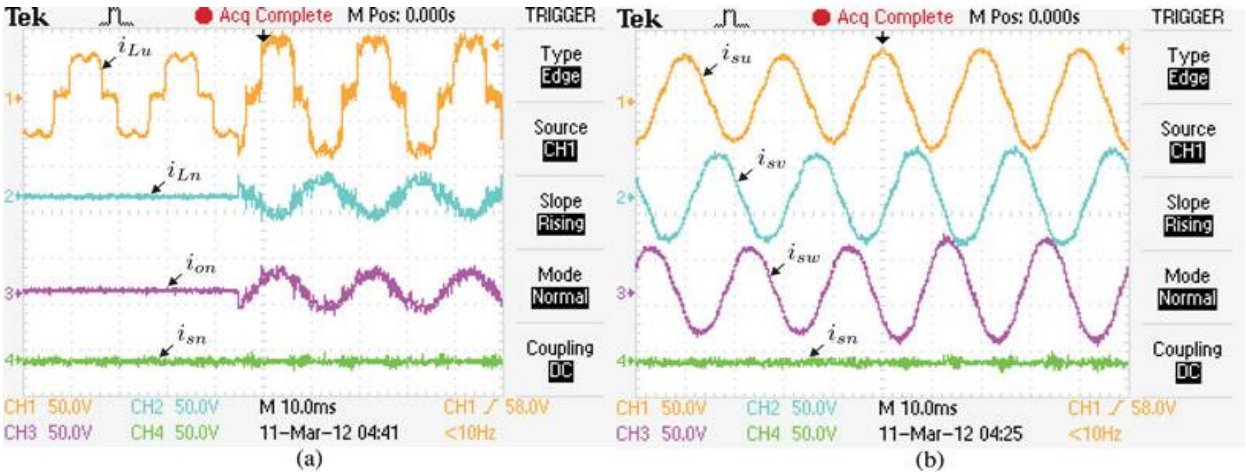

Figure. 11. Experimental results for step unbalanced phase u load change (1.0 to 1.3 p.u.). (a) Load Current *iLu*, load neutral current *iLn*, active power filter neutral current *ion* , and system neutral current *isn*. (b) System currents *isu* ,*isv* , *isw*, and *isn*.

The corresponding waveforms are shown in Fig. 11. Fig. 11(a) shows that the active filter is able to compensate the current in the neutral conductor with fast transient response.

Moreover, Fig. 11(b) shows that the system neutral current *i*on is effectively compensated and eliminated, and system currents remain balanced even if an 11% current imbalance is applied.

VI .EXTENSION RESULTS USING FUZZY CONTROLLER

Fuzzy logic is both old and new because, although the modern and methodical science of fuzzy logic is still young, the concept of fuzzy logic relies on age-old skills of human reasoning. By using the fuzzy logic controller we can decrease the fluctuations and also decreases the imbalance currents.When comparing with the pi controller the fuzzy controller mostly decreases the voltage and imbalance currents of the active power filter.The fuzzy controller was replaced by the pi controller in matlab function in subsystem. the below results are when we are using the fuzzy controller we can decrease the voltage and load currents as shown in Fig.12.

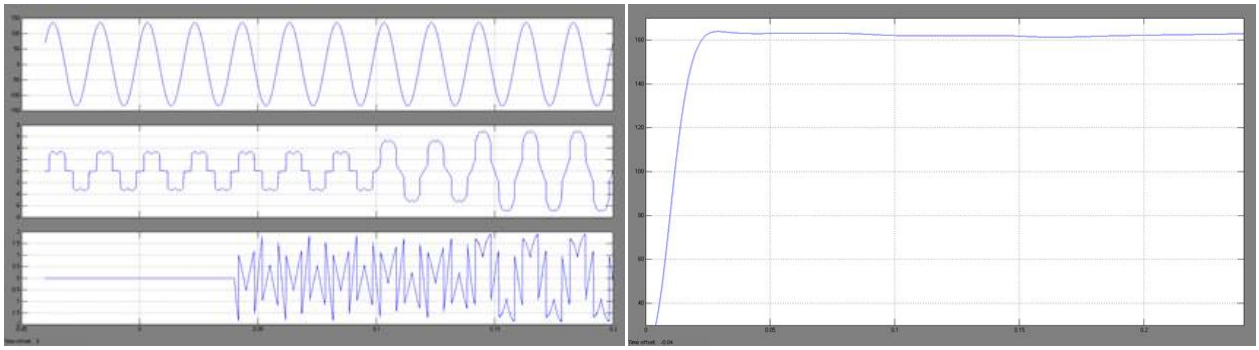

(a) Phase current (b) Load current

Figure. 12 .Experimental results for(a) phase and (b)Load current

VII. CONCLUSION

Improved dynamic current harmonics and a reactive power compensation scheme for power distribution systems with generation from renewable sources has been proposed to improve the current quality of the distribution system. Advantages of the proposed scheme are related to its simplicity, modeling, and implementation. The use of a

ISSN (Print) : 2320 – 3765
ISSN (Online): 2278 – 8875

International Journal of Advanced Research in Electrical, Electronics and Instrumentation Engineering

(An ISO 3297: 2007 Certified Organization)

Vol. 5, Issue 6, June 2016

predictive control algorithm for the converter current loop proved to be an effective solution for active power filter applications, improving current tracking capability, and transient response. Simulated and experimental results have proved that the proposed predictive control algorithm is a good alternative to classical linear control methods. The predictive current control algorithm is a stable and robust solution. Simulated and experimental results have shown the compensation effectiveness of the proposed active power filter.

REFERENCES

[1] S. Kouro, P. Cortes, R. Vargas, U. Ammann, and J. Rodriguez, "Model predictive control—A simple and powerful method to control power converters," *IEEE Trans. Ind. Electron.*, vol. 56, no. 6, pp. 1826–1838, Jun. 2009.
[2] M. Karimi-Ghartemani, S. Khajehoddin, P. Jain, A. Bakhshai, and M. Mojiri, "Addressing DC component in PLL and notch filter algorithms," *IEEE Trans. Power Electron.*, vol. 27, no. 1, pp. 78–86, Jan. 2012.
[3] T. Geyer, "Computationally efficient model predictive direct torque control," *IEEE Trans. Power Electron.*, vol. 26, no. 10, pp. 2804–2816, Oct. 2011.
[4] M. Rivera, C. Rojas, J. Rodriidguez, P. Wheeler, B. Wu, and J. Espinoza, "Predictive current control with input filter resonance mitigation for a direct matrix converter," *IEEE Trans. Power Electron.*, vol. 26, no. 10, pp. 2794–2803, Oct. 2011.
[5] Z. Shen, X. Chang, W. Wang, X. Tan, N. Yan, and H. Min, "Predictive digital current control of single-inductor multiple-output converters in CCM with low cross regulation," *IEEE Trans. Power Electron.*, vol. 27, no. 4, pp. 1917–1925, Apr. 2012.
[6] D. Quevedo, R. Aguilera, M. Perez, P. Cortes, and R. Lizana, "Model predictive control of an AFE rectifier with dynamic references," *IEEE Trans. Power Electron.*, vol. 27, no. 7, pp. 3128–3136, Jul. 2012.
[7] R. de AraujoRibeiro, C. de Azevedo, and R. de Sousa, "A robust adaptive control strategy of active power filters for power-factor correction, harmonic compensation, and balancing of nonlinear loads," *IEEE Trans. Power Electron.*, vol. 27, no. 2, pp. 718–730, Feb. 2012.
[8] J. Rocabert, A. Luna, F. Blaabjerg, and P. Rodriguez, "Control of power converters in AC microgrids," *IEEE Trans. Power Electron.*, vol. 27, no. 11, pp. 4734–4749, Nov. 2012.

BIOGRAPHY

M.B.Hemanthkumarpresently working as Assistant professor in the Dept. of Electrical and Electronics Engineering from Annamacharya Institute of Technology and Science –Hyderebad.He has completed M.Tech from Annamacharya Institute of Technology and Sciences-Rajampet(Autonomous) in the year 2015 and completed B.Tech from Siddharth Institute of Engineering and Technology-Puttur.He is presently doing research on Wind turbine systens and area of interest are renewable energy, Distributed systems.

M.Chandrashekhar presently working as as Assistant professor in the Dept. of Electrical and Electronics Engineering from Annamacharya Institute of Technology and Science –Hyderebad.His area of research are renewable energy, Fuzzy controller, Power converters.